



HAL
open science

Fast Soft Tissue Deformation and Stump-Socket Interaction Toward a Computer-Aided Design System for Lower Limb Prostheses

A. Ballit, I. Mougharbel, H. Ghaziri, T.-T. Dao

► **To cite this version:**

A. Ballit, I. Mougharbel, H. Ghaziri, T.-T. Dao. Fast Soft Tissue Deformation and Stump-Socket Interaction Toward a Computer-Aided Design System for Lower Limb Prostheses. *Innovation and Research in BioMedical engineering*, 2020, 41, pp.276 - 285. 10.1016/j.irbm.2020.02.003 . hal-03492171

HAL Id: hal-03492171

<https://hal.science/hal-03492171>

Submitted on 17 Oct 2022

HAL is a multi-disciplinary open access archive for the deposit and dissemination of scientific research documents, whether they are published or not. The documents may come from teaching and research institutions in France or abroad, or from public or private research centers.

L'archive ouverte pluridisciplinaire **HAL**, est destinée au dépôt et à la diffusion de documents scientifiques de niveau recherche, publiés ou non, émanant des établissements d'enseignement et de recherche français ou étrangers, des laboratoires publics ou privés.



Distributed under a Creative Commons Attribution - NonCommercial 4.0 International License

Fast Soft Tissue Deformation and Stump-Socket Interaction toward a Computer-Aided Design System for Lower Limb Prostheses

Abbass Ballit¹, Imag Mougharbel², Hassan Ghaziri³, Tien-Tuan Dao¹

abbass-khodor.ballit@utc.fr, imadmoug@yahoo.com, hassan.ghaziri@gmail.com, tien-tuan.dao@utc.fr

¹Sorbonne University, Université de Technologie de Compiègne, CNRS, UMR 7338 Biomechanics and Bioengineering, Centre de Recherche Royallieu, CS 60 319 Compiègne, France

²École de Technologie Supérieure de Montréal, Groupe de Recherche en Électronique de Puissance et Commande Industrielle, Québec, Canada

³Beirut Research and Innovation Center (BRIC), Beirut, Lebanon

Corresponding author: Tien Tuan Dao, Ph.D.

Sorbonne University, Université de Technologie de Compiègne, CNRS UMR 7338

Biomechanics and Bioengineering

CS 60319, 60203 Compiègne cedex, France

Tel: 33 3 44 23 43 34

E-mail: tien-tuan.dao@utc.fr

Abstract

Prosthetic technology is rapidly advancing but there's a catch. Regardless the technology or the material used, a minimum cost is still high. One of the problems relates to the fact that the conventional socket fabrication process is still used. This method is based on subjective estimations of the involved specialists and feedbacks of the patients. This process consumes remarkable amount of time, manpower and materials. Research works are needed to design new efficient and low-cost alternative techniques for the socket design. This technique should definitely be based on CAD-CAM methods. Therefore, the first step toward this objective is to establish an accurate numeric model for evaluating and optimizing the design process. In this present work, we developed a new approach to simulate the stump soft tissue deformation and stump-socket interaction using Mass-Spring System (MSS) approach and a point-to-surface contact formulation.

A novel Mass-Spring System with corrective spring (MSS-CS) model was developed and evaluated. A node-to-surface contact formulation was also integrated and evaluated. The MSS-CS model and contact formulation were evaluated with primitive geometrical object and a stump-socket model. Moreover, a finite element model of the stump-socket interaction was also developed using Abaqus to evaluate the proposed approach.

Obtained results show that the proposed contact formulation has a very good precision level and the contact pressures on the interface between the elastic and rigid bodies are very close to the analytical solutions. The comparison with Abaqus showed a qualitative concordance for the contact pressure. However, quantitative deviation remains high [25-50] % at the peak contact pressure due to different contact formulations. In particular, our MSS-CS approach is more efficient than Abaqus simulation in term of computational time and cost.

A novel approach was proposed to model soft tissue deformation and stump-socket interaction in an efficient and accurate manner. As perspectives, this present approach for a real-time simulation of the stump-socket interaction could be used in a real-time CAD-CAM platform to provide a cost-effective socket manufacturing process.

Keywords: *Lower Limb Prosthesis, Soft Tissue Deformation, Stump-Socket interaction, Mass-Spring Model, CAD System.*

I. INTRODUCTION

Lower-limb prostheses are generally developed with three main parts: the socket, the pylon (leg section), and the foot. In particular, the socket is considered as an important element in the design process of the prosthesis. Note that each socket is a tailor-made product designed to fit with the unique geometry of the patient's residual limb [1]. A poorly fitting socket can cause significant trauma. Current practice in the design and fabrication of a prosthetic socket usually starts by creating a wrap cast of the residual limb, which is filled by plaster to form the positive mold of the stump (Figure 1). Using his experience, the prosthetist applies some modifications to the positive mold before a socket is formed over it. These modifications aim to produce the expected pressure distribution on the stump/socket interface during usage of the prosthesis. During the fitting stage, the socket is usually modified several times until achieving a well-fit socket. The decision is based on the feedbacks of the patient and the personal judgement of the involved specialist. This process is time-consuming and expensive requiring incremental refinements for the final prototype of the socket, and especially its accuracy depends strongly on the expertise of a high cost specialist [2]. All these elements lead to the unaffordable high prices of the final products: a simple lower limb prosthesis that allows its user to simply stand and walk in level ground costs between 5000\$ and 7000\$ [3], and even the most expensive ones are built to withstand only three to five years of wear and tear, meaning they will need to be replaced over the course of a lifetime. Therefore, an alternative effective low-cost socket design and fabrication process is needed in order to reduce the incredibly high price of these products.



Figure 1: Current practice in the fabrication of the prosthetic socket

Many researches have been conducted for improving the socket design and fabrication process using Computer-Aided-Design approach. In 2007, Bonacini et al. [4] proposed a socket design process where all phases are computer-aided, but they focused on the reconstruction of the stump model. They analyzed 3 different technologies to obtain the geometry model of the stump, which are based on laser scanning to acquire external geometry of the stump, and computer tomography (CT) and magnetic resonance imaging (MRI) for the inner parts. This study did not consider other steps of the process. Another computer-aided process was proposed by Hsu et al. in 2010 [5] to design and develop the prosthetic socket. This process follows the same steps of the conventional method but using manual 3D modeling tools. However, this study does not help to overcome the need of repetitive modifications, the subjectivity and high production time and cost. Frillici et al., in 2008 [6], introduced the role of finite element (FE) simulation to innovate the prosthesis design process. However, only feasibility study with preliminary results was reported. In 2013, a virtual environment to design and test lower limb prosthesis has been proposed by Colombo et al [7]. The VSL (Virtual Socket Laboratory) consists of a "Socket Modeling Assistance" system where the prosthetist can model the socket using manual 3D modeling tools, starting from the 3D geometry of the stump. This modeling method is assisted by FE simulation of interaction between the designed socket and the stump. The residual limb model is obtained from MRI scan and physical parameters derived from previous works are applied to the soft tissues. This FE model has been evaluated in another article published in 2016 [8], where the simulation results were compared to experimental ones. Note that FE simulation of the stump-socket system has been commonly performed in other studies [9] [10] [11] to predict the pressure distribution on the stump-socket interface and make quantitative evaluation of the socket design. Overall, these previous works have several common limitations. The first drawback relates to the very high computational cost of the used finite element method, making it difficult to perform fast dynamic simulations. Moreover, the contact formulation in finite element theory is complex and inappropriate for a fast feedback to correct the design of the socket. In fact, previous works did not mention any idea about the integration of their models into a real-time CAD-CAM platform, as efficient alternative for the conventional design and fabrication process. Consequently, in this present

study, we developed a new approach to simulate the stump soft tissue deformation and stump-socket interaction using Mass-Spring System (MSS) approach and a point-to-surface contact formulation.

II. MATERIALS AND METHODS

II.1. SOFT TISSUE DEFORMATION

A. Mass-Spring System Configuration

Our approach is based on the use of the Mass-Spring System (MSS) applied on hexahedral mesh. Using the MSS model, an elastic object is represented by a set of punctual masses, called nodes. Each node is defined by its mass and its position vector, connected together by elastic connections as shown in Figure 2. A stiffness k , a damping coefficient c , an initial length L_0 , and the two point masses are also defined. This model corresponds to the Kelvin-Voigt model for the viscoelastic material.

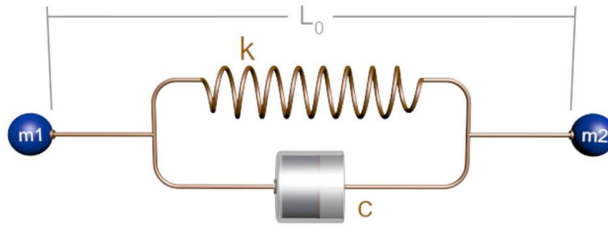


Figure 2: Schematic representation of the connection between 2 punctual masses.

The distribution of the nodes in the volume of the modeled object is managed by the type of mesh used. In our present study, we used the hexahedral mesh. This choice has been justified by the fact that the hexahedral mesh gives better response to shear stresses than tetrahedral mesh [17]. However, this model, illustrated in Figure 3(a), has the potential to react correctly to normal compression forces but not to shearing forces, since the springs do not have shear properties. To overcome this limitation, the hexahedral element allows us to benefit from its 4 internal diagonals as well as the 12 diagonals of these faces. The use of these diagonals as elastic connections, in a well definite way, shows their ability to keep several important properties: the shear, and the non-compressibility properties of the soft tissues. Figure 3(b) shows a regular hexahedral element with the 28 possible elastic connections between its 8 nodes. Note that the hexahedral element is considered as linear elastic model defined by its Young's modulus and density.

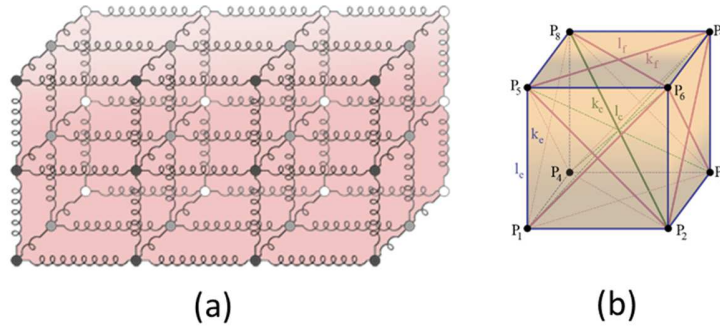


Figure 3: (a) Hexahedral MSS model and (b) hexahedral element with the 28 possible connections: 12 edge connections in blue, 12 faces diagonals in red, and 4 internal diagonals in green

B. Parameters Identification

After having the shape subdivision (meshing) and MSS configuration established, the parameters (the mass of each vertex, the stiffness and damping coefficient of each connection) of each item in the model are identified. To find the mass m_i of a vertex i , we used the following formula presented by Deussen et al. [19] as follows:

$$m_i = \frac{1}{8} \sum_H \rho_j V_j \quad (1)$$

where H is the group of hexahedral elements to which the vertex i belongs, ρ_j and V_j are the density and volume of the hexahedral element j that belongs to H respectively.

The stiffness of each spring was calculated using the formulation presented in [20]. Reference to the hexahedral element shown in the figure 2, there are 3 types of connections (edges, internal diagonals, face diagonals) with stiffness constants k_e , k_c and k_f respectively. The values of these parameters were identified using the following formulations:

$$\begin{cases} \frac{k_f}{k_c} = A \\ k_c = \frac{3El_e}{10+7.5A} = \frac{\sqrt{3}El_c}{10+7.5A} \\ k_f = \frac{1.5AEl_e}{10+7.5A} = \frac{1.5AEl_f}{\sqrt{2}(10+7.5A)} \\ k_e = \frac{0.75AEl_e}{10+7.5A} + \frac{2El_e}{10+7.5A} \end{cases} \quad (2)$$

where E is the young modulus assigned to the hexahedral element, and l_e is the length of its edge considering that this is a regular cubical element. A is a parameter to be manually tuned. Golec [20] proved that the model shows the same results for any given value to A between 0.1 and 100. If a connection is shared by multiple hexahedral elements, its stiffness is equal to the sum of the corresponding quantities calculated for each hexahedral element according to the equation 2.

Finally, to ensure the best behavior consistency for different and combined resolutions [20] [21] [22] [23], the damping coefficient c_i of a spring of index i and stiffness k_i connecting two punctual masses m_{i1} and m_{i2} with initial length l_{i0} , are expressed in the following equation:

$$c_i = \frac{2\sqrt{k_i(m_{i1}+m_{i2})}}{l_{i0}} \quad (3)$$

C. Volume Conservation

Soft tissues are incompressible materials, i.e. their volume remains constant under external and internal loadings. For this kind of material, the Poisson's Modulus tends to 0.5, while the system defined in equation 2 deals only with a Poisson's modulus equal to 0.25 [17] [20]. To solve this problem, a novel approach, called MSS-CS (Mass-Spring System Corrective Springs), was developed in this study. In fact, additional springs, named "Corrective Springs" were integrated to the MSS model. Thus, the proposed configuration consists of adding, in parallel with the internal diagonal springs with stiffness k_c and initial length l_c (resp. the face diagonal springs with stiffness k_f and initial length l_f), new springs having stiffness k'_c and initial length l'_c (resp. stiffness k'_f and initial length l'_f). Constitutive equations of our MSS-CS are based on the following two conditions, which are described below.

Condition 1: The initial lengths of these additional springs are greater than the initial geometric lengths as follows:

$$\frac{l'_c}{l_c} = \frac{l'_f}{l_f} = \alpha \quad \text{with } \alpha > 1 \quad (4)$$

This condition allows added springs to be always extended to conserve the volume (Figure 4).

Condition 2: The stiffness of each of these springs is calculated in terms of the volume variation as follows:

$$\delta v = \frac{V_c - V_0}{V_0} \quad (5)$$

where V_0 and V_c are the initial and actual volume of the hexahedral element respectively.

The corrective spring's stiffness is defined as follows:

$$k'_f = k'_c = C E l_e (\delta v)^3 \quad (6)$$

where C is a constant to be identified.

Supposing that the hexahedral element is regular, i.e. a cube, then:

$$l_e = \sqrt[3]{V_0} \quad (7)$$

Therefore:

$$k'_f = k'_c = C E \sqrt[3]{V_0} \left(\frac{V_c - V_0}{V_0}\right)^3 \quad (8)$$

Finally, our proposed model is then characterized by the equations (2), (4) and (8), with three constants $A = 0.5$; $C = 25$; $\alpha = \sqrt{2}$.

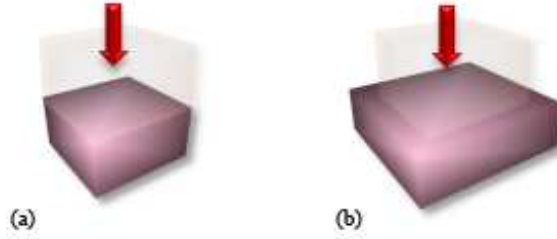


Figure 4: Cubical elastic object subject to normal compression pressure: (a) Compressible material modeled using MSS without corrective springs. (b) Uncompressible material modeled using MSS with corrective springs performing horizontal expansion to conserve its

D. Simulation Algorithm

Let N be the total number of vertices in the MSS-CS model. Two types of forces are applied on each vertex of index i : internal forces, noted F_{int}^i , applied by the related elastic connections, and external forces, noted F_{ext}^i . Let m_i and a_i be the mass and acceleration of the vertex i respectively. Then, according to the second law of Newton, the equilibrium equation is defined as follows:

$$F_{int}^i + F_{ext}^i = m_i a_i \quad (10)$$

Knowing that the internal forces are spring and damping forces calculated in terms of the position X_i and its first derivative X'_i respectively, and that a_i is equal to the second derivative X''_i , we need to apply an integration on the equation (10) to find the new position of the vertex i in each simulation step Δt . We chose the implicit Euler integration method that gives a more stable simulation than the explicit one. A first order linearization is performed since the forces are non-linear according to the position variable. Applying these steps on all N vertices of the system, we get a system of $3N$ linear equations with $3N$ unknowns. The matrix of such system is always symmetric positive definite. Therefore, we can solve the system using Conjugate Gradient method.

II.2. STUMP-SOCKET INTERACTION

A. Socket modeling

To simplify the implementation and reduce the computational cost, the socket is considered as a rigid body. Usually, sockets are made of perlon stockinette hardened by resin, which makes it firmly stiff and non-deformable. Beside its triangular 3D surface (Figure 5), the rigid socket is characterized by the following physical parameters: mass M_s , moment of inertia I_s , center of mass C_M , and center of inertia C_s . The behavior of the socket in the 3D space is described by the following second law of Newton:

$$\vec{F}_s = M_s \vec{a}_s \quad \text{and} \quad \vec{\tau}_s = I_s \vec{\omega}_s \quad (11)$$

where F_s is the sum of all forces applied to the socket, τ_s is the sum of all torques applied to the socket, a_s and ω_s are the acceleration and angular speed of the socket.

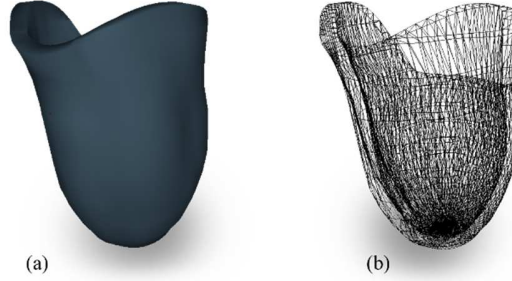


Figure 5: 3D triangular surface of a transtibial prosthetic socket (a) shaded view, (b) wireframe view

B. Contact modeling

Modeling contact between two 3D objects includes two numerical processing components: 1) a collision detection algorithm and 2) a formulation of physical response.

1) Collision detection algorithm

A node-to-triangle discrete collision detection algorithm was established. In this method, a collision occurs when the point penetrates into the triangle, i.e. it passes through the triangle from the positive side of the triangle's plane to the negative one (Figure 6).

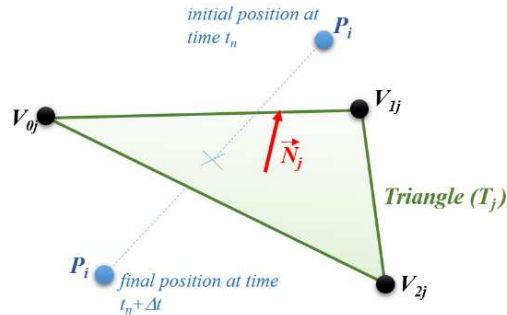


Figure 6: Schematic representation of the collision taking place between the point P_i and the triangle T_j

Thus, in each simulation time-step, the involved point is checked to verify if this point is behind the triangle's plane and whether its orthogonal projection to this plane is inside the triangle (Figure 7). In other words, we trace a ray from the point in the 3D space and verify whether it intersects with the triangle and whether the point is behind this triangle. Noting that, in our method, the ray is to be parallel to the triangle's normal vector. Practically, a collision occurs between a point P_i of the stump and a triangle T_j of the socket if these following equations are true:

$$\begin{cases} \overrightarrow{V_{0j}P_i} \cdot \vec{N}_j \leq 0 \\ 0 \leq u \leq 1 \\ 0 \leq v \leq 1 \\ 0 \leq u + v \leq 1 \end{cases} \quad (12)$$

where V_{0j} , V_{1j} , V_{2j} are the three points of the triangle T_j . u and v are the barycentric coordinates of the projection Pr_{ij} of the point P_i with respect to the triangle T_j . These coordinates define the position of the projection point with respect to the three triangle's vertices as follows:

$$Pr_{ij} = V_{0j} + u(V_{1j} - V_{0j}) + v(V_{2j} - V_{0j}) \quad (13)$$

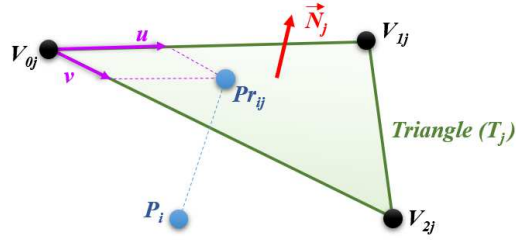


Figure 7: collision detected between the point P_i and the triangle T_j

In the equation (12), the first inequality means that the point is behind the triangle. The remaining three inequalities confirm that the projection point to the triangle's plane is inside the triangle. If all these inequalities are true, the point P_i and the triangle T_j are considered as "contact pair". In case if these conditions are satisfied between P_i and multiple triangles, the nearest triangle to the point is selected.

Basically, the test is applied between each point of the stump surface and each triangle of the socket. Having N points and M triangles, the complexity in this case will be $O(N \times M)$, which increases exponentially when the resolution of meshes increases. The final step in the collision detection phase is placing the point of each contact pair on a well selected collision-free position. In our method, we choose the projection of this point to the triangle as the corrected position.

2) Formulation of physical response

Physical response or reaction of the collision consists of all the forces applied to the socket and the stump due to the collision. Basically, this mechanical reaction consists of two types of forces: the normal contact force, and the friction force. According to the third law of Newton, the forces applied to the elements of the contact pair are equal in magnitude and opposite in direction. Thus, having selected N_c contact pairs in the first phase, for each contact pair C_k ($k \in \{1, 2, 3, \dots, N_c\}$), the point P_k and the triangle T_k are each subject to a contact force of magnitude F_{cont}^k and a friction of magnitude F_{fric}^k . Thus, the force applied by the point of the stump surface to the contact surface of the socket is equal to the sum of the inner forces \vec{F}_{int,P_k} applied to the point due to the material mechanical properties along with the external forces \vec{F}_{ext,P_k} . This total force applied to the point is noted \vec{F}_{P_k} and expressed in the following equation:

$$\vec{F}_{P_k} = \vec{F}_{int,P_k} + \vec{F}_{ext,P_k} \quad (14)$$

Talking about a normal contact force, we will consider the forces perpendicular to the triangle and disregard the forces aligned with it. Therefore, the magnitude of the contact force is defined as follows:

$$F_{cont}^k = -\vec{F}_{P_k} \cdot \vec{N}_K \quad (15)$$

The minus sign in the equation (15) is added to obtain a positive value, since the force \vec{F}_{P_k} applied to the point should be pushing the triangle, having opposite direction of the triangle normal vector \vec{N}_K (Figure 8(a)).

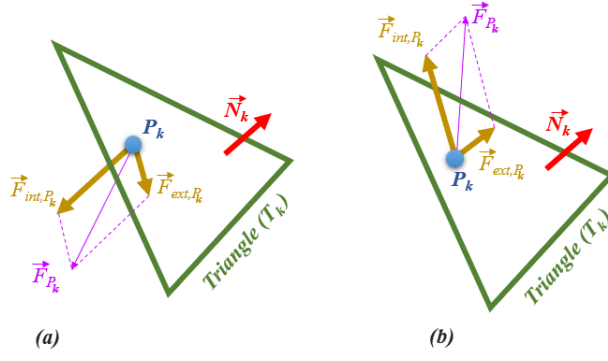


Figure 8: (a) Forces applied to the point are toward the triangle, so the contact force exists. (b) The forces applied to the point are not toward the triangle, so no contact force is considered

In the opposite case, if this equation gives a negative value, this would mean that the point is “pulled” instead of being “pushed” by the internal and external forces (Figure 8(b)). In this case, we discard it and set the contact force to null. Finally, the vectors of contact forces \vec{F}_{cont,P_k} and \vec{F}_{cont,T_k} applied to the point P_k and the triangle T_k respectively are defined as follows:

$$\begin{cases} \vec{F}_{cont,P_k} = F_{cont}^k \cdot \vec{N}_k \\ \vec{F}_{cont,T_k} = -F_{cont}^k \cdot \vec{N}_k \end{cases} \quad (16)$$

Once a contact force exists between the contact pair elements, the friction force is computed. This force basically depends on the relative velocity between the two elements. Let \vec{V}_k be the relative velocity vector of the point P_k moving with a velocity \vec{V}_{P_k} with respect to the triangle T_k moving with a velocity \vec{V}_{T_k} :

$$\vec{V}_k = \vec{V}_{P_k} - \vec{V}_{T_k} \quad (17)$$

If this relative velocity is null, the friction is ignored, otherwise, its magnitude is defined as follows:

$$F_{fric}^k = \mu F_{cont}^k \quad (18)$$

where μ is the friction coefficient assigned to the stump-socket interface. The direction of the friction vector \vec{F}_{fric,P_k} applied to the point is opposite to its relative velocity vector. The friction vector \vec{F}_{fric,T_k} applied to the triangle is in the other direction as follows:

$$\begin{cases} \vec{F}_{fric,P_k} = -F_{fric}^k \cdot \frac{\vec{V}_k}{\|\vec{V}_k\|} \\ \vec{F}_{fric,T_k} = F_{fric}^k \cdot \frac{\vec{V}_k}{\|\vec{V}_k\|} \end{cases} \quad (19)$$

The forces generated by the collision between the elements of each contact pair are thus calculated. To introduce them into the simulation, we apply the following steps:

Step 1: For each point P_k of the contact pair C_k and existing on the surface of the stump model, the contact force \vec{F}_{cont,P_k} and the friction \vec{F}_{fric,P_k} are added to the external forces in equation (10).

Step 2: Regarding the socket, two vectors are necessary to simulate its behavior in the 3D space: the total force \vec{F}_s and the total torque $\vec{\tau}_s$, as shown in the equation (11). The total force is simply found by summation of the forces applied to the triangles T_k , $k \in \{1, 2, 3, \dots, N_c\}$, along with any other external force $\vec{F}_{S,ext}$ applied to the socket as follows:

$$\vec{F}_s = \vec{F}_{S,ext} + \sum_{k=1}^{N_c} (\vec{F}_{cont,T_k} + \vec{F}_{fric,T_k}) \quad (20)$$

For the torque, let first consider for each contact pair C_k a torque $\bar{\tau}_k$ that is generated by the interaction of P_k and T_k and defined as follows:

$$\bar{\tau}_k = (\vec{F}_{cont,T_k} + \vec{F}_{fric,T_k}) \cdot \overrightarrow{P_k C_I} \quad (21)$$

where C_I is the center of inertia of the socket. The total torque is then the summation of all these particular torques with any other external torque $\bar{\tau}_{s,ext}$ that may exist:

$$\bar{\tau}_s = \bar{\tau}_{s,ext} + \sum_{k=1}^{N_C} \bar{\tau}_k \quad (22)$$

II.3. SIMULATION ENVIRONMENT DEVELOPMENT

A simulation environment was developed by using C++ programming language. Graphical user interface was designed and developed with “Visual Studio / Windows Form Application”. OpenGL library [35] was used for the 3D visualization. A virtual transtibial residual limb was developed using the available CAD model library (free3D.com) (Figure 9(a)). A hexahedral mesh of the model (Figure 9(b)) was generated using the open-source tool IA-FEMesh [36], from which the code automatically generates the related MSS-CS model (Figure 9(c)) and calculate its parameters from the predefined physical parameters of the soft tissues. A Young’s modulus of 50KPa [8], [37] was used. The density for soft tissue was set up as 1060Kg/m³ [38].

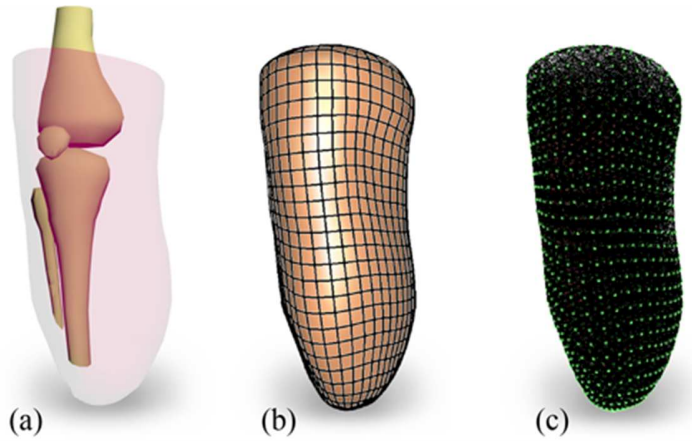


Figure 9: Stump model: (a) original 3D model, (b) hexahedral mesh, (c) MSS-CS model

A geometrical process was developed to create the socket model (Figure 5). Stump geometry was used to extrapolate the socket geometry with a thickness of 10 mm. Finally, the soft tissue deformation and stump-socket interaction algorithms were integrated into the developed environment.

II.4. ACCURACY ANALYSIS

Two simulation cases were developed to evaluate the accuracy of our soft tissue deformation and stump-socket interaction algorithms. We started first by a simple cubical elastic object subject to normal compression due to the weight of a rigid box (Figure 10). We repeated the simulation with different weight values, and we recorded, for each one, the displacement and contact pressure on elastic cube’s upper surface as well as its volume variation, and we compared them to analytical results. We also implemented the MSS-CF model developed by Golec [20] for comparison. The dimensions of the elastic cube are 50mm. Young’ modulus of 50KPa and a density of 1060Kg/m³ were used.

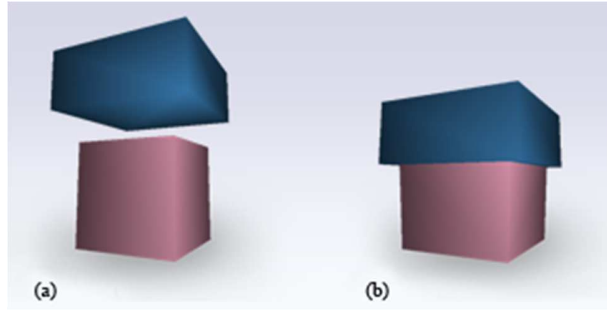


Figure 10: Compression of the pink elastic cube due to the weight of the blue rigid box: (a) initial state, (b) final state

In the second case, we performed a dynamic simulation for the socket donning process (Figure 11), and we mapped the contact pressure distribution on the stump-socket interface. The same physical properties (Young' modulus of 50KPa and a density of 1060Kg/m³) were assigned to the stump soft tissues. The socket moves according to a displacement constraint.

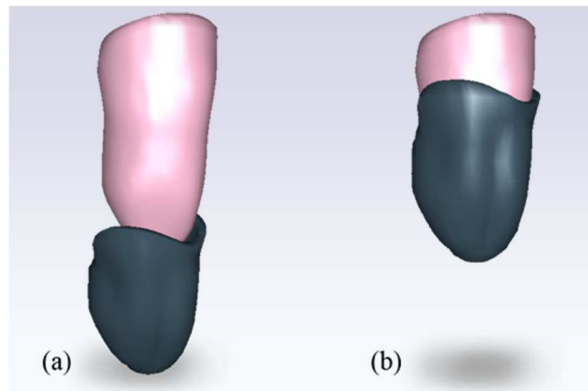


Figure 11: Schematic simulation of the socket donning process: (a) initial state, (b) final state

Finally, a FE model of the stump-socket interaction was developed using Abaqus for the comparison with our MSS-CS model. A C++ code was written to convert the MSS-CS model to an Abaqus model, so that the same meshes are used in both simulations. A convergence analysis was conducted to determine the optimal mesh configuration (7393 nodes of which 778 are related to the bones and are fixed, and 6270 hexahedral elements (Figure 12)) of the involved models. The same physical properties (Young' modulus of 50KPa and a density of 1060Kg/m³) were assigned to the stump soft tissues. A Poisson ratio of 0.45 was used [39]. All parameters used in the FE simulation are given in table 1. The simulation was performed on an HP workstation with 16GB RAM and Intel® Core™ i7-7700HQ 2.8GHz CPU.

	<u>Parameters</u>	<u>Values</u>
Stump	Young's modulus	50 KPa
	Poisson ratio	0.45
	Density	1060 Kg/m ³
Socket	Young's modulus	50 000 N/m ²
	Poisson ratio	10 GPa
	Density	500 Kg/m ³
	Gravity	9.8 m/s ²
Step	Type	Dynamic, Implicit
	Time Period	1 s
Contact	Interaction type	Surface-to-Surface contact
	Normal behavior	Hard contact
	Tangential behavior	Frictionless

Table 1: Parameters of the FE simulation performed by Abaqus

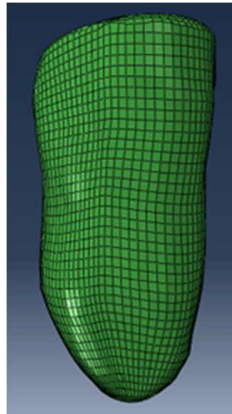


Figure 12: Optimal meshed stump model used in socket donning simulation

III. RESULTS

A. Cubical elastic object simulation

Contact pressure, displacement ratio and volume tracking of the cubical elastic object are shown in Figures 13, 14 and 15. Obtained results show that the MSS-CF is very accurate regarding volume conservation but does not reflect the real linear elastic behavior with error reaching 20% for a displacement of 5%, compared to the analytical results. In other hand, our MSS-CS approach shows more satisfying elastic behavior with errors that don't exceed 5% for up to 50% displacement. Even though the Figure 15 shows that the MSS-CS is not as efficient as the MSS-CF regarding the volume conservation, we consider it acceptable with error equal to 3.1% for 10% displacement. Figure 13 confirms that our contact model has a very good precision level and the contact pressures on the interface between the elastic and rigid bodies are very close to the analytical solutions. These simulations were performed in real time and the average calculation time of each time step is equal to 15.29 μ s.

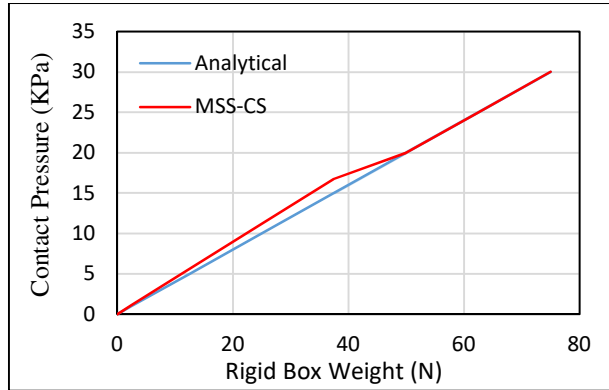


Figure 13: Contact pressure on the upper surface of the elastic cube in function of the rigid box weight

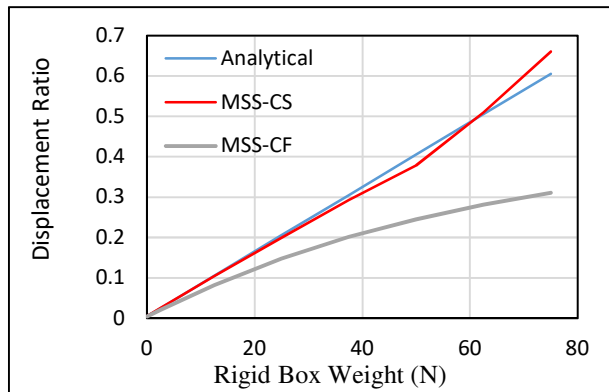


Figure 14: Displacement ratio of elastic cube upper surface in function of the rigid box weight

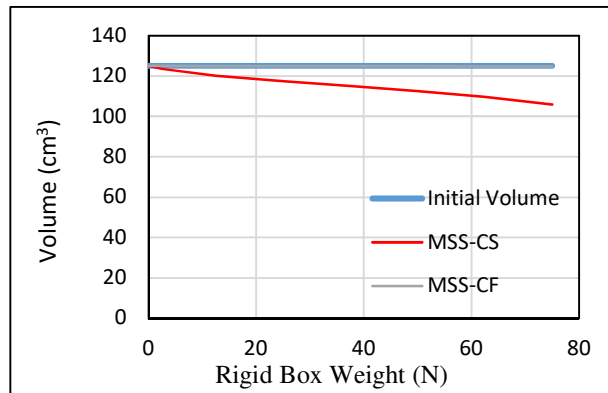


Figure 15: Volume of elastic object in function of applied weight

B. Stump-socket interaction simulation

The results shown in the Figure 16 were captured at the end of the socket donning process simulation by using Abaqus software and our MSS-CS approach. Overall, the two pressure patterns have a satisfactory correspondence in a qualitative manner. To make a quantitative evaluation, two profiles were tracked on the front vertical line as shown in figure 17(a), and those existing on the circumference of a circle as shown in figure 17(b). The first points set has been chosen since the line cut a critical point in the stump, the patellar tendon, and the points are represented by their height, i.e. z coordinate. The second point set has been chosen in a way to evaluate the pressure on tabular flares as well as medial, lateral and posterior pressure zones. We represented these points by their angular coordinate with respect to the vertical axis passing through the middle of the stump. The contact pressure distributions for these 2 points set are given in Figures 18 and 19. We observed a very good fitting pattern between our MSS-CS approach and Abaqus simulation. However, a relative error ranging from 25% to 50% was found at the peak contact pressure. In addition, the simulation time using

Abaqus is around 5 hours 25 minutes and 10 second, while our simulation time is around 69 seconds. Although the simulation time is considerably reduced, the real time simulation is not reached because of a time step reduction for assuring simulation stability. The time step was set to 1ms while it's needed calculation time was equal to 69ms almost divided equally between the stump deformation calculation and the contact calculation (30ms and 33.9ms respectively, and the rest is for rendering and other calculations).

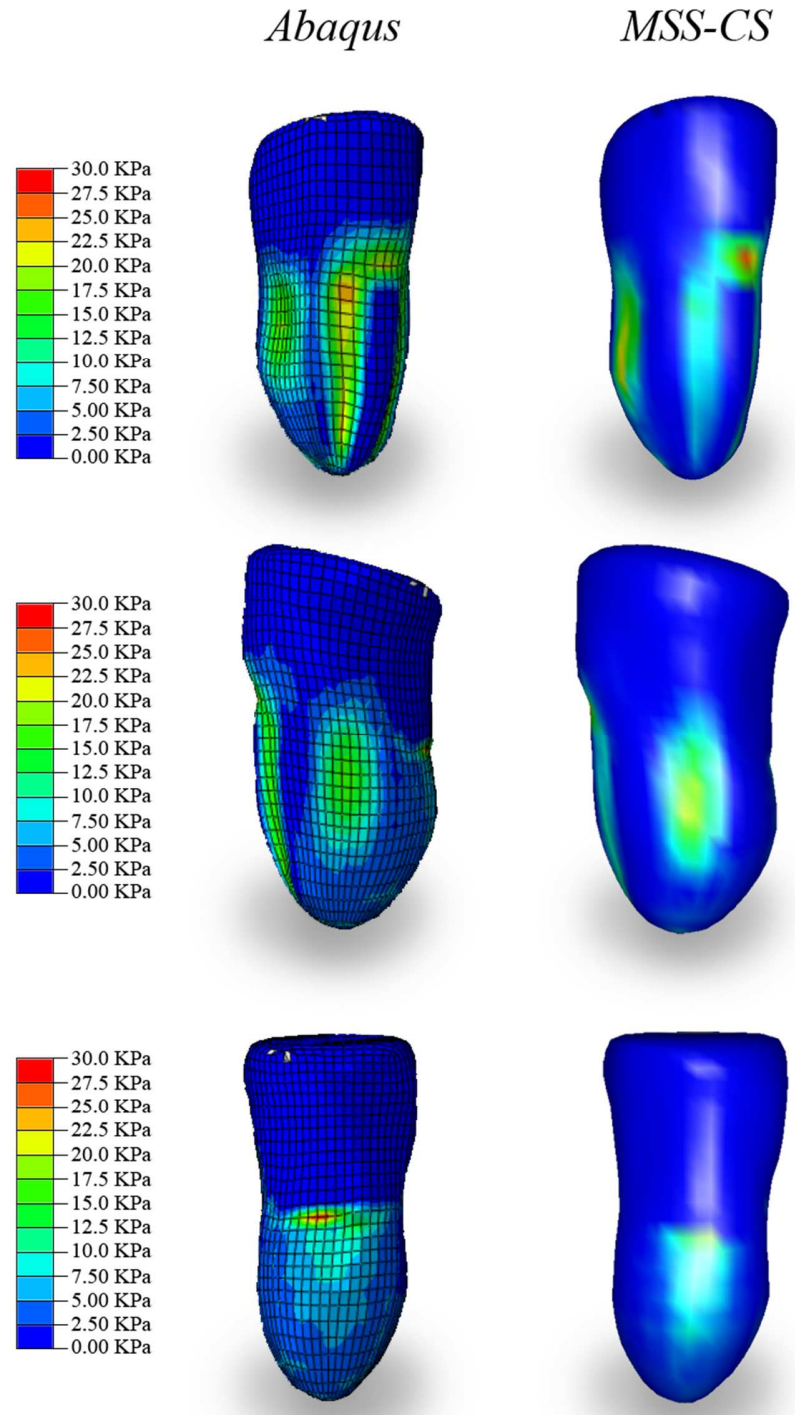


Figure 16: Contact pressure distribution on the stump-socket interface from both MSS-CS and FE simulations at the end of the socket donning process

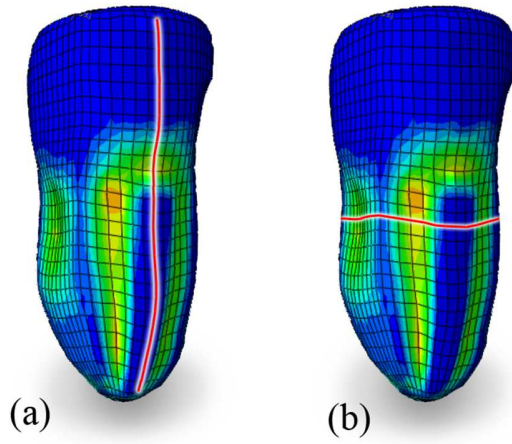


Figure 17: the two points sets chosen for quantitative evaluation

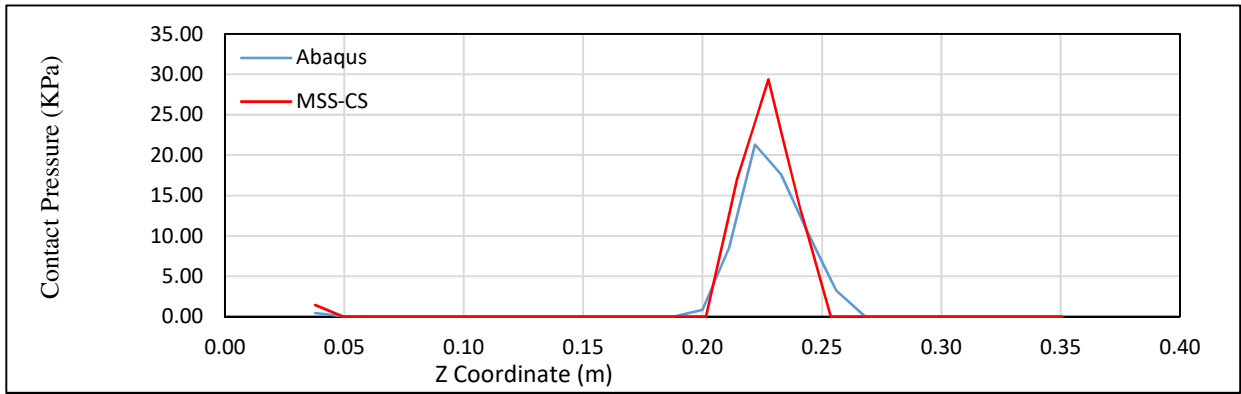


Figure 18: Contact pressure distribution on the vertical points set

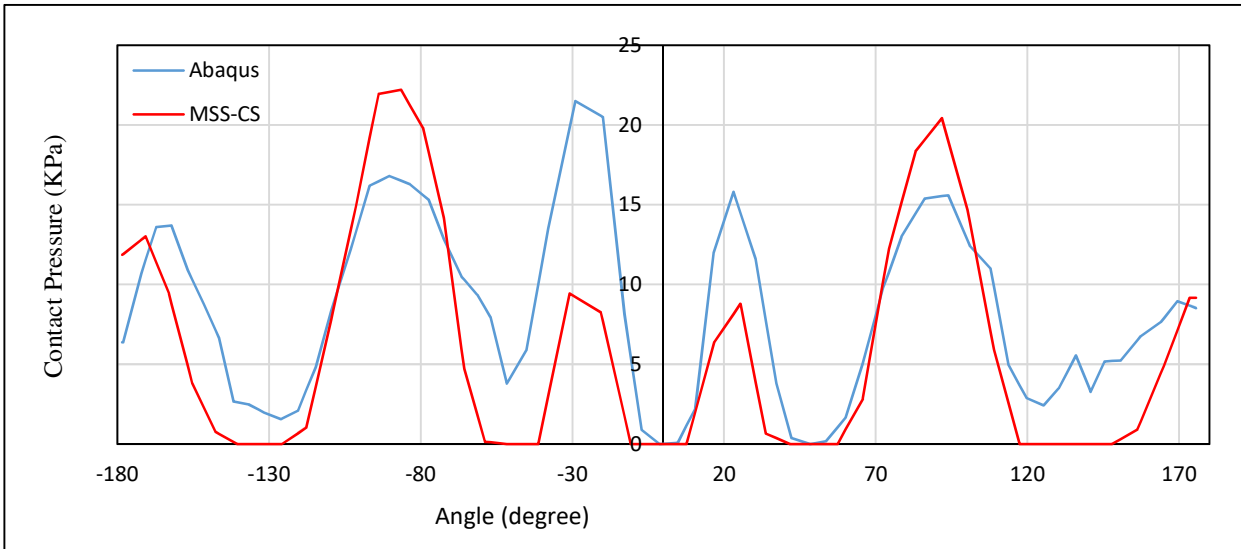


Figure 19: Contact pressure distribution on the horizontal points set

IV. DISCUSSION

Prosthesis design has become an attractive field in the recent years thank to the progress of 3D printing capacity and biomechanical researches. However, traditional manual design and fitting process has been commonly performed in many

hospitals and clinics over the world. This time-consuming and inefficient process leads to a high medical cost and requires significantly human resources [2]. Research studies have been conducted to improve this process. Virtual prototyping studies have been proposed. Numerical modeling based on finite element methods has been usually used to provide objective and quantitative indicators for evaluating and optimizing the design process [7] [8] [9] [10] [11]. Even if FE-based approach leads to a detailed level of feedback, simulation outcomes require significantly computational resources and complex modeling skills. To deal with this problem, in this present study, a novel approach was proposed to estimate the soft tissue deformation and stump-socket interaction during the design process. A Mass-Spring System coupled with corrective springs (MSS-CS) was developed and evaluated according to a finite element model. Thanks to its simplicity and low computational cost, MSS-based approach attracts the interest of many researchers in different domains to model the elastic objects like in video games and computer graphics [12] [13] [14] as well as in surgical simulators [15] [16] where researchers work on developing virtual training environment. Unfortunately, the literature analysis shows that this approach is not yet introduced in the prosthetic domain. This approach was adopted in this study to provide a more efficient computational approach for soft tissue deformation. Regarding the MSS-based studies, many researchers proposed to add a new type of forces to each vertex, called “Corrective Forces”, which are functions of Poisson’s modulus and volume variation. Inspired by previous works, Golec [20] proposed a formulation of these volume correction forces, giving a new model called MSS-CF (Mass-Spring System Corrective Forces). Golec’s results showed the validity of these additional forces to perfectly correct the volume but did not show their impact on the elastic behavior. In this study, we already showed that MSS-CF model would negatively impact the elastic response of the model to an applied stress. We noticed that the problem resides in the direction of the resistive forces to an applied stress when the material is compressed. By comparing to this approach, our MSS-CS showed more consistent and accurate results (shown in Figure 14).

In addition, a formulation of stump-socket contact was also proposed in this study. Collision detection (CD) is the computational problem of detecting the geometric intersection of objects in the 3D space. Many CD methods for rigid and deformable bodies have been proposed and used in different applications such as video games [24], robotics [25], surgical simulators [26] [27] [28]. Generally speaking, there are two basic types of collision detection algorithms: discrete collision detection (DCD) and continuous collision detection (CCD). DCD detects the collision between the two objects in a discrete time, so the exact collision time is missed, and the detection is made after the penetration of an object into the other. The collided items then are moved to corrected collision-free positions. In other hand, CCD searches for the exact collision moment in the interval bounded by two time-steps. It has been proposed for collision between rigid bodies [29] [30] and then used for detection of self-collision of deformable objects [31] [32]. CCD is more robust than DCD but requires very high computational cost, while the latter is much simpler and cheaper. Usually, it is extremely difficult to compare the different collision detection methods and choose one of them since they are very sensitive to specific scenario [33]. In our case, a high simulation speed is required, that’s why the DCD approach was used. More precisely, an algorithm derived from ray-casting-based method proposed by Fukuhara et al. in 2014 [34] was developed with few modifications (inverse way of collision (deformable object to rigid one) and ignorance of false contact pairs) to make it compatible with our application. By comparing with a detailed finite element contact simulation, our formulation gives a similar contact behavior with a perfect qualitative matching. However, quantitative deviation of contact pressure at peak values remains high. Note that this quantitative difference may be due to the different contact formulations between Abaqus (surface-to-surface contact) and our approach (point-to-surface contact). Thus, further studies will be investigated to improve our contact formulation. Even if our MSS-CS is more efficient than Abaqus simulation in term of computational time, our computation cost remains high. A possible simple solution to reduce the calculation time is to automatically assign to each point, at the beginning of the simulation, the potential contact triangle, so the algorithm will test each point with the assigned triangles only. For instance, we remarked that the points of the posterior aspect of the stump never collide with the triangles in front of the socket. In addition, all triangles of the external surface of the socket can be discarded. Thus, further studies will be investigated to improve this point.

Another limitation of our study relates to the use of linear elastic material to model soft tissue. However, this simplification is considered acceptable in our application because the deformations of stump soft tissues are small and within the linear region. Previous work [18] experimented both linear and hyper-elastic models, and results show similar pressure distribution for both cases but a considerably higher simulation speed in case of linear model.

V. CONCLUSIONS AND PERSPECTIVES

A novel approach was proposed to model soft tissue deformation and stump-socket interaction toward a Computer-Aided Design (CAD) system for lower limb prostheses. A Mass-Spring System Corrective Spring (MSS-CS) model was developed and

evaluated. Nonlinear “Corrective” springs were introduced to respect the non-compressibility of the soft tissues. A node-to-surface contact formulation was also integrated and evaluated. Obtained results confirmed the efficiency and accuracy of the proposed method comparing to a complex and detailed finite element model. As perspectives, this present approach will be used to simulate the stump-socket interaction in real case studies. Thus, the evaluation of the proposed approach will be enhanced with more datasets. Finally, this modeling approach will be integrated into a CAD-CAM platform providing a fast feedback to the prosthetist during the socket manufacturing process.

ACKNOWLEDGMENT

The authors would like to acknowledge the support and funding of “Beirut Research and Innovation Center” (BRIC), Beirut, Lebanon.

REFERENCES

- [1] N. Herbert, D. Simpson, W. D. Spence, W. Ion, “A Preliminary Investigation into the Development of 3-D Printing of Prosthetic Sockets”, *JRRD*, Vol.42, N.2, March/April 2005, p.141-146.
- [2] Leandro Lorenzelli, et al.” Socketmaster: Integrated Sensors System for the Optimised Design of Prosthetic Socket for above Knee Amputees”, Published in: CAS (NGCAS), 2017 New Generation of, 6-9 Sept. 2017, pp. 233-236.
- [3] McGimpsey, G., Bradford, T., 2010. *Limb Prosthetics Services and Devices*. Bioengineering Institute Center for Neuroprosthetics, Worcester Polytechnic Institution, Worcester, MA
- [4] Bonacini, D., Corradini, C. & Magrassi, G. 2007, 3-D Digital Model Reconstruction: Residual Limb Analysis to Improve Prosthesis Design. In A. Gruen & H. Kahmen (eds.), *Optical 3-D Measurement Techniques VIII*. Zurich, Switzerland.
- [5] Hsu LH, Huang G, Lu CT, Hong DY, Liu SH (2010) The development of a rapid prototyping prosthetic socket coated with a resin layer for transtibial amputees. *Prosthet Ortho Int*34(1):37–45
- [6] Frillici FS, Rissone P, Rizzi C, Rotini F. 2008 The role of simulation tools to innovate the prosthesis socket design process. In *Intelligent production machines and system* (eds DT Pham, EE Eldukhri, AJ Soroka), pp. 612-619. Dunbeath, UK: Whittles Publishing.
- [7] Colombo G, Facoetti G, Rizzi C. 2013 A digital patient for computer-aided prosthesis design. *Interface Focus* 3: 20120082. [http:// dx.doi.org/10.1098/rsfs.2012.0082](http://dx.doi.org/10.1098/rsfs.2012.0082)
- [8] Colombo, Giorgio & Comotti, Claudio & Redaelli, Davide & Regazzoni, Daniele & Rizzi, Caterina & Vitali, Andrea. (2016). A Method to Improve Prosthesis Leg Design Based on Pressure Analysis at the Socket-Residual Limb Interface. 10.1115/DETC2016-60131.
- [9] F. V. Waldenfels, S. Raith, M. Eder, A. Volf, J. Jalali, L. Kovacs, “Computer Assisted Optimization of Prosthetic Socket Design for the Lower Limb Amputees Using 3-D Scan”, 3rd International Conference on 3D Body Scanning Technologies, Lugano, Switzerland, 16-17 October 2012
- [10] Surapureddy, Rajesh, "Predicting Pressure Distribution Between Transfemoral Prosthetic Socket and Residual Limb Using Finite Element Analysis" (2014).UNF Theses and Dissertations.Paper 551.
- [11] Cagle J. C., Reinhall P. G., Allyn K. J., McLean J., Hinrichs P., Hafner B. J., et al. . (2018). A finite element model to assess transtibial prosthetic sockets with elastomeric liners. *Med. Biol. Eng. Comput.* 56, 1227–1240. 10.1007/s11517-017-1758-z
- [12] J. Bender, D. Koschier, P. Charrier, D. Weber: "Position-Based Simulation of Continuous Materials". *Computer & Graphics*. (2014)
- [13] J. Bender, M. Müller, M. Macklin: "Position-Based Simulation Methods in Computer Graphics". *NVIDIA PhysX Research*. (2015)
- [14] T. Liu, S. Bouaziz, L. Kavan: "Quasi-newton methods for real-time simulation of hyperelastic materials". *ACM Trans. Graph.* 36, 3, Article 23 (May 2017)
- [15] François Goulette, Zhuo-Wei Chen. Fast computation of soft tissue deformations in real-time simulation with Hyper-Elastic Mass Links. *Computer Methods in Applied Mechanics and Engineering*, Elsevier. (2015)
- [16] L. Xu, Y. Lu, Q. Liu: "Integrating viscoelastic mass-spring-dampers into position-based dynamics to simulate soft tissue deformation in real time", *R.Soc.open sci.*5:171587. (2018)

- [17] V. Baudet, M. Beuve, F. Jaillet, B. Shariat, and F. Zara. "Integrating Tensile Parameters in Hexahedral Mass-Spring System for Simulation". In: WSCG'2009. 2009. ISBN: 9788086943930
- [18] Colombo, G., Facoetti, G., Morotti, R., and Rizzi, C., 2011, "Physically based modelling and simulation to innovate socket design", *Computer-Aided Design and Applications*, 8 (4), pp. 617-631.
- [19] Oliver Deussen, Leif Kobbelt, and Peter Tücke. "Using Simulated Annealing to Obtain Good Nodal Approximations of Deformable Bodies". In: *Computer Animation and Simulation '95: Proceedings of the Eurographics Workshop in Maastricht, The Netherlands, September 2-3, 1995*. Ed. by Demetri Terzopoulos and Daniel Thalmann. Vienna: Springer Vienna, 1995, pp.30-43. ISBN: 978-3-7091-9435-5. DOI:10. 1007/978-3-7091-9435-5_3
- [20] Karolina Golec. "Hybrid 3D Mass Spring System for Soft Tissue Simulation. Modeling and Simulation". Université de Lyon, 2018. English. <NNT: 2018LYSE1004>. <tel-01761851v2>
- [21] Paloc, C., Bello, F., Kitney, R., Darzi, A.: Online multiresolution volumetric mass spring model for real time soft tissue deformation. In: *Medical Image Computing and Computer Assisted Intervention*. pp. 219-226 (2002)
- [22] B. A. Lloyd, G. Székely, and M. Harders. "Identification of spring parameters for deformable object simulation". In: *IEEE Transactions on Visualization and Computer Graphics* 13.1 (2007), pp. 1081-1093. ISSN: 10772626. DOI: 10.1109/TVCG.2007. 1055.
- [23] Y. Duan, W. Huang, H. Chang, W. Chen, K. K. Toe, J. Zhou, T. Yang, J. Liu, S. K. Teo, C. W. Lim, Y. Su, C. K. Chui, S. Chang: "Modeling and Simulation of Soft Tissue Deformation". *International MICCAI Workshop on Computational and Clinical Challenges in Abdominal Imaging, ABD-MICCAI*. pp 221-230 (2013)
- [24] Ericson C (2004) *Real-time collision detection*. CRC Press, Boca Raton
- [25] Balan L, Bone GM (2006) Real-time 3D collision avoidance method for safe human and robot coexistence. In: *Intelligent Robots and Systems, 2006 IEEE/RSJ International Conference on*. IEEE, pp 276-282
- [26] Courtecuisse H, Jung H, Allard J, Duriez C, Lee DY, Cotin S (2010) Gpu-based real-time soft tissue deformation with cutting and haptic feedback. *Prog Biophys Mol Biol* 103(2):159-168
- [27] Malone HR, Syed ON, Downes MS, D'Ambrosio AL, Quest DO, Kaiser MG (2010) Simulation in neurosurgery: a review of computer-based simulation environments and their surgical applications. *Neurosurgery* 67(4):1105-1116
- [28] F. Fazioli, F. Ficuciello, G. A. Fontanelli, B. Siciliano, L. Villani, "Implementation of a soft-rigid collision detection algorithm in an open-source engine for surgical realistic simulation", *Proc. IEEE Int. Conf. Robot. Biomimetics*, pp. 2204-2208, 2016.
- [29] Redon S, Kheddar A, Coquillart S (2002) Fast continuous collision detection between rigid bodies. In: *Computer Graphics Forum*, vol 21. Wiley Online Library, pp 279-287
- [30] Kim B, Rossignac J (2003) Collision prediction for polyhedral under screw motions. In: *Proceedings of the Eighth ACM Symposium on Solid Modeling and Applications*. ACM, New York, USA, pp 4-10
- [31] Brochu T, Edwards E, Bridson R (2012) Efficient geometrically exact continuous collision detection. *ACM Trans Graph (TOG)* 31(4):96
- [32] Liang He , Ricardo Ortiz , Andinet Enquobahrie , Dinesh Manocha, Interactive continuous collision detection for topology changing models using dynamic clustering, *Proceedings of the 19th Symposium on Interactive 3D Graphics and Games*, February 27-March 01, 2015, San Francisco, California [doi>10.1145/2699276.2699286]
- [33] Trenkel S, Weller R, Zachmann G. A benchmarking suite for static collision detection algorithms. In: *Int. conf. in central Europe on computer graphics, visualization and computer vision*. 2007
- [34] A. Fukuhara, T. Tsujita, K. Sase, A. Konno, X. Jiang, S. Abiko, M. Uchiyama, "Proposition and evaluation of a collision detection method for real time surgery simulation of opening a brain fissure", *ROBOMECH Journal*, vol. 1, no. 6, 2014.
- [35] OpenGL Architecture Review Board, SHREINER D., WOO M., NEIDER J., DAVIS T.: *OpenGL Programming Guide: The Official Guide to Learning OpenGL*. Addison-Wesley, 2003
- [36] Grosland NM, Shivanna KH, Magnotta VA, Kallemeyn NA, DeVries NA, Tadepalli SC, Lisle C., IA-FEMesh: An open-source, interactive, multiblock approach to musculoskeletal finite element model development, *Comput Methods Programs Biomed* 2009 Apr;94(1):96-107.

- [37] B. C. W. Kot, Z. J. Zhang, A. W. C. Lee, V. Y. F. Leung, S. N. Fu: "Elastic Modulus of Muscle and Tendon with Shear Wave Ultrasound Elastography: Variations with Different Technical Settings". *PLoS One*. 7(8): e44348. (2012)
- [38] Urbancheka, M; Picken, E; Kalliainen, L; Kuzon, W (2001). "Specific Force Deficit in Skeletal Muscles of Old Rats Is Partially Explained by the Existence of Denervated Muscle Fibers". *The Journals of Gerontology Series A: Biological Sciences and Medical Sciences*. 56 (5): B191–B19
- [39] Chawla A, Mukherjee S, Karthikeyan B (2006) Mechanical properties of soft tissues in the human chest, abdomen and upper extremities

